Impact of climate on landscape form, sediment transfer and the sedimentary record

Received: 1 July 2020 | Revised: 8 January 2021 | Accepted: 12 January 2021

DOI: 10.1002/esp.5075

RESEARCH ARTICLE

ESPL WILEY

Impact of climate on landscape form, sediment transfer and the sedimentary record

Rebekah M. Harries[1,2] | Boris Gailleton[1] | Linda A. Kirstein[1] | Mikael Attal[1] | Alexander C. Whittaker[3] | Simon M. Mudd[1]

[1]School of GeoSciences, The University of Edinburgh, Edinburgh, UK

[2]Research Centre for Integrated Disaster Risk Management, Pontifical Catholic University of Chile, Santiago, Chile

[3]Royal School of Mines, Imperial College London, UK

Correspondence
Rebekah M. Harries, CIGIDEN Centro de Investigación para la Gestión Integrada del Riesgo de Desastres, Campus San Joaquín, Pontificia Universidad Catolica de Chile, Vicuña Mackenna 4860, Macul, La Florida, Región Metropolitana.
Email: rebekah.harries@cigiden.cl

Funding information
European Union initial training, Grant/Award Number: 674899 - SUBITOP; Research Center for Integrated Disaster Risk Management (CIGIDEN), Grant/Award Number: ANID/FONDAP/15110017; The School of Geosciences at The University of Edinburgh; NERC E3 DTP studentship, Grant/Award Number: NE/L002588/1

Abstract

The relationship between climate, landscape connectivity and sediment export from mountain ranges is key to understanding the propagation of erosion signals downstream into sedimentary basins. We explore the role of connectivity in modulating the composition of sediment exported from the Frontal Cordillera of the south-central Argentine Andes by comparing three adjacent and apparently similar semi-glaciated catchment-fan systems within the context of an along-strike precipitation gradient. We first identify that the bedrock exposed in the upper, previously glaciated reaches of the cordillera is under-represented in the lithological composition of gravels on each of three alluvial fans. There is little evidence for abrasion or preferential weathering of sediment sourced from the upper cordillera, suggesting that the observed bias can only be explained by sediment storage in these glacially widened and flattened valleys of the upper cordillera (as revealed by channel steepness mapping). A detailed analysis of the morphology of sedimentary deposits within the catchments reveals catchment-wide trends in either main valley incision or aggradation, linked to differences in hillslope–channel connectivity and precipitation. We observe that drier catchments have poor hillslope–channel connectivity and that gravels exported from dry catchments have a lithological composition depleted in clasts sourced from the upper cordillera. Conversely, the catchment with the highest maximum precipitation rate exhibits a high degree of connectivity between its sediment sources and the main river network, leading to the export of a greater proportion of upper cordillera gravel as well as a greater volume of sand.

Finally, given a clear spatial correlation between the resistance of bedrock to erosion, mountain range elevation and its covariant, precipitation, we highlight how connectivity in these semi-glaciated landscapes can be preconditioned by the spatial distribution of bedrock lithology.

These findings give insight into the extent to which sedimentary archives record source erosion patterns through time.

KEYWORDS
channel steepness, climate, connectivity, glaciation, landscape evolution, sediment storage, sedimentary record

1 | INTRODUCTION

Sediment export from mountain ranges controls the morphodynamic behaviour of lowland rivers (Baynes et al., 2020; Pfeiffer et al., 2019) as well as the physical characteristics of their sedimentary records (Quick et al., 2019; Watkins et al., 2020). An understanding of the controls on sediment export is therefore essential for constraining how river systems, and their associated hazards, have and will respond to changes in their climatic or tectonic boundary conditions (Micheletti & Lane, 2016).

It has often been assumed that sediment export occurs relatively instantaneously and is therefore proportional to erosion and sediment production rates in upstream catchments (Allen, 2008; Castelltort & Van Den Driessche, 2003; Molnar, 2004). In source regions, erosion rates are modulated by bedrock lithology and precipitation rates, which are expected to be recorded in the gradient of hillslopes and the steepness of river channels (Hurst et al., 2013; Johnstone & Hilley, 2015; Roda-Boluda et al., 2018). All else being equal, a landscape experiencing uniform erosion is expected to display steeper slopes where rocks are more resistant to erosion or where precipitation is lower, with steeper slopes providing the increase in erosion potential needed to counterbalance the effect of greater rock strength or deficit in discharge, respectively (D'Arcy & Whittaker, 2014; Kirby & Whipple, 2012; Zondervan et al., 2020). On this basis, one might assume that the stratigraphic record preserved downstream of such mountain ranges will have a lithological composition that reflects upstream bedrock erosion rates and thus can be used to reconstruct the lithological and tectonic evolution of the sediment routing system (Amidon et al., 2005a, 2005b). Indeed this assumption is at the root of cosmogenic and thermochronology techniques for estimating catchment-averaged rates of bedrock erosion (10^{2-5} years) and bedrock exhumation (> 10^6 years), respectively (Delunel et al., 2020; Kirstein et al., 2010; Reinhardt et al., 2007; Riesner et al., 2019; von Blanckenburg, 2005).

While it is expected that sediment production is dependent on the tectonic, lithologic and climatic drivers controlling landscape form, modelling (Tofelde et al., 2019), experimental (Jerolmack & Paola, 2010) and field studies (Clapp et al., 2000) have shown that sediment export has a more complex relationship with the geomorphological evolution of the sediment routing system. This is particularly evident in landscapes that have experienced glaciation. In glaciated landscapes, erosion can vary spatially, often focused in two distinct zones along valley profiles (Figure 1): the first, in the headwaters, where bedrock quarrying results in the back-wearing of head walls, and the second, proximal to the Equilibrium Line Altitude, where abrasion smooths valley floors (MacGregor et al., 2000) (Figure 1). Such a mechanism can reduce the concavity of longitudinal river profiles (Brocklehurst & Whipple, 2002). It can also widen valleys and increase hillslope erosion through the de-buttressing of steepened slopes upon glacier retreat (Ballantyne, 2002). A number of studies have reported that sediment yields from post-glacial catchments are heavily influenced by sediment storage in wide, low gradient reaches over a range of timescales (Brardinoni et al., 2018; Church & Ryder, 1972; Harbor & Warburton, 2006; Malatesta et al., 2018). Malatesta et al. (2018) recognised that these reaches act as sediment flux capacitors, which modulate the release of sediment downstream as a function of water and sediment discharge.

A number of field studies have recognised that, while climate wetness is a critical driver of sediment export, differences in the timing of sediment delivery and terrace aggradation on piedmonts is fundamentally linked to temporal variability in landscape connectivity (Malatesta & Avouac, 2018; Norton et al., 2016; Schildgen et al., 2016). Here, landscape connectivity is defined by how easily sediment can be mobilised both longitudinally, along the length of a river network and between hillslopes and channels, thereby influencing the efficiency of landscapes in storing sediment (Hooke, 2003; Jerolmack & Paola, 2010; Li et al., 2016; Molnar, 2001; Rainato et al., 2018). Longitudinal connectivity can be modulated by, for example, bed slope and grain size thresholds in sediment transport, which can differ between river reaches (Whitbread et al., 2015). Connectivity between hillslopes and the river network is modulated by catchment geometry, river planform, hillslope morphology and hillslope processes (Mishra et al., 2019; Norton et al., 2016). While connectivity may be established in one part of the sedimentary system, it can have negative feedbacks elsewhere along its length (Korup et al., 2010; Lane et al., 2017; Rainato et al., 2018). For example, in the Humahuaca basin of NW Argentina, Schildgen et al. (2016) documented differences in the timing of terrace aggradation in response to an increase in precipitation-induced landsliding. They suggested that the propagation of the precipitation-induced landslide flux to the downstream alluvial system was dependant on whether or not the increased hillslope activity, as well as the basin's shape, promoted temporary damming of the river network. In the Tian Shan, Malatesta et al. (2018) documented differences in the amplitude of piedmont aggradation and incision cycles in response to a period of increased precipitation. Cycle amplitudes were found to be higher downstream of catchments that had been partially glaciated in their upper reaches, when compared with catchments that were entirely glaciated or strictly fluvial. They related this trend to longitudinal dis-connectivity along the river network of semi-glaciated catchments.

It is known that both hillslope–channel and longitudinal connectivity are driven by water discharge but limited by sediment supply (Tofelde et al., 2019). The evolution of connectivity along the length

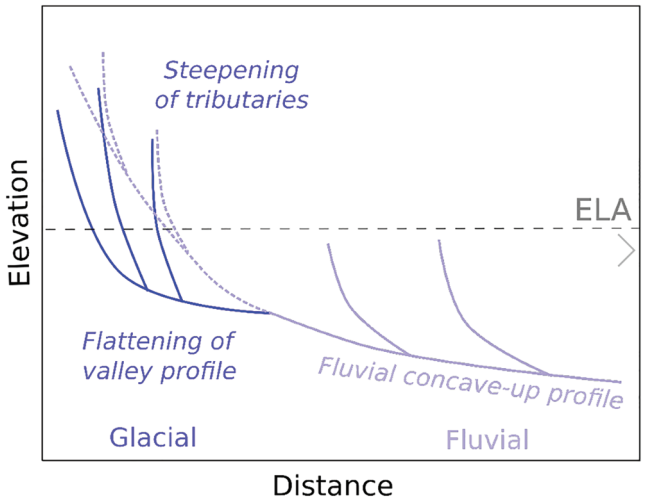

FIGURE 1 Conceptual model of how glacial erosion influences the longitudinal profile of river networks, adapted from MacGregor et al. (2009). From a strictly fluvial profile (dashed line), over-deepening of the main valley by glacial erosion reduces its steepness while increasing that of tributaries and headwaters

of coupled mountain–basin river systems and how it impacts sediment export, however, is still largely undocumented. Filling this research gap is critical if we are to have a better understanding of how sedimentary systems and their associated hazards will evolve in response to future climatic change.

In this contribution, we examine to what extent the lithologic and climatic controls on landscape form are translated downstream into the composition of sediments deposited on three adjacent alluvial fans. In comparing three apparently similar catchment-fan systems, we observe the role of connectivity in modulating sediment export from semi-glaciated catchments, within the context of an along-strike precipitation gradient.

2 | STUDY AREA

The Frontal Cordillera of the Andes between 30°S and 31°S was uplifted during the Neogene as one of a number of east-verging structures activated by the progressive shallowing of plate subduction (Figure 2) (Gonzalez et al., 2020; Jordan et al., 1993; Martinod et al., 2020; Ramos et al., 2002). Thick-skinned deformation of Palaeozoic basement created the high topography of the Frontal Cordillera during a main stage of uplift in the late Miocene between ~9.5 and 4.5 Ma (Jordan et al., 1993), which generated 2 ± 1 km of relief (Hoke et al., 2014). Since ~5 Ma, active shortening has migrated to the eastern Precordillera and to the Pampean range, leaving the Frontal Cordillera and western Precordillera influenced primarily by strike-slip fault activity (Siame et al., 1997). The current tectonic stability of this region makes the Andean cordillera at 30–31°S a good location to investigate the impact of lithologic and climatic forcing on landscape evolution.

In this study, we focus on five adjacent catchments, east of the Frontal Cordillera drainage divide, which feed three alluvial fans in the Iglesia basin (Harries et al., 2018, 2019). The Palaeozoic basement exposed in these catchments is composed of two dominant lithological units of similar age (Figure 2a). The upper cordillera is composed of a sequence of volcaniclastic units from the Early Permian–Triassic, comprising tuff, ignimbrites and agglomerates interbedded with limestone. The lower cordillera is composed of a predominantly fluvial sequence of sedimentary units including sandstones, conglomerates, limestone and marine shales making up the Silurian–Early Permian Agua Negra Formation. This formation is intruded by granites emplaced during the Permian–Triassic (Jones et al., 2016). The highest peaks in the cordillera are capped with the Late Pliocene–early Pleistocene Olivares basalt in the south, and elsewhere by Oligocene–Miocene volcanic rocks, predominantly andesite and rhyolite, from the Cerro de las Tortolas and Dona Ana formations, which are associated with the El Indio–Pascua belt exposed to the west of the

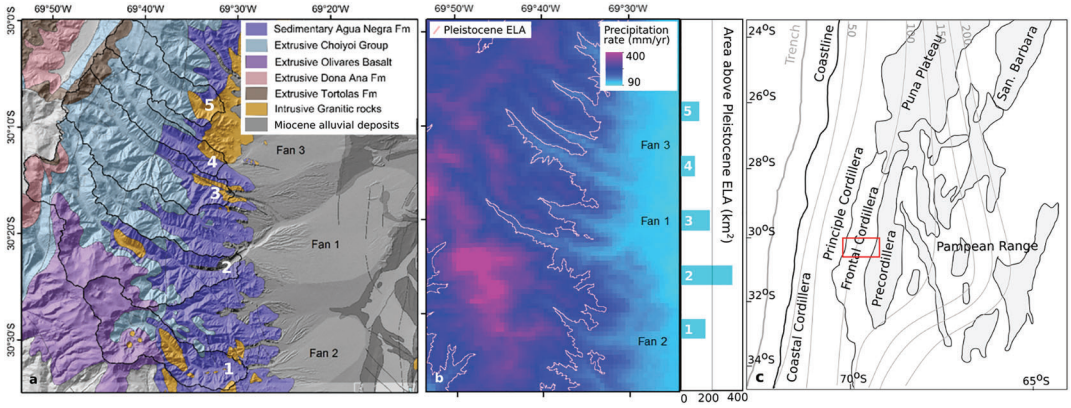

FIGURE 2 (a, b): Study location in the Argentine Andes, 30–31°S, South America, including delineation of the three catchment-fan systems studied (fans labelled 1–3 with contributing catchments labelled 1–5). (a) Geological map. (b) Spatial distribution of annual precipitation averaged for the period 1970–2000. Here we include the Pleistocene (pink) equilibrium line altitude (ELA), at 4000 m asl (Clapperton, 1994) and plot the catchment area in km^2 above 4,000 m for each catchment. (c) Location of study site with respect to main tectonic units, including isobaths of the subducted oceanic slab, adapted from Ramos et al., (2002)

drainage divide (Jones et al., 2016). The clear differentiation between the volcanic/volcaniclastic rocks exposed in the upper cordillera and sedimentary rocks in the lower cordillera allows sediment sourced from these two regions to be distinguished. This is useful as the boundary between these two units is exposed at the approximate elevation of the Pleistocene Equilibrium Line Altitude (ELA), ~4,000 m (Clapperton, 1994), and therefore, broadly speaking, identifies volcanic reaches as formerly glaciated, while sedimentary reaches of the lower cordillera were not. There are no terminal moraines preserved at this latitude to verify glacial extent (D'Arcy et al., 2019), however the altitude of the Pleistocene ELA can be extrapolated from the altitudes of terminal moraines preserved in nearby valleys, notably the Rio Aconcagua, Rio Mendoza and Elqui valleys. This ELA reconstruction is supported by observations of the relationship between elevation and precipitation gradients, snowline altitudes and the distribution of glaciers, in this region (Clapperton, 1994).

The climate in this mountain range is semi-arid and therefore lends itself to the study of physical surface processes given the absence of extensive vegetation (cf. Jeffery et al., 2014). While rivers here are ephemeral and are predominantly supplied by glacier and snow melt throughout the spring, extreme precipitation events, often associated with the El Niño Southern Oscillation, have an important role in sediment transport (Perucca & Martos, 2012), as observed in both flash flood events and in the Quaternary sedimentary record of this region (Colombo et al., 2009). The present ELA in the studied catchments is ~5,000 m (Figure 2b), peak elevations increase from 5,000 to 6,000 m in the south, where glaciers are larger and more abundant (Harries et al., 2018). This trend in elevation is mirrored in precipitation rates which are on average 100 mm/year higher in the south than in the north. This latitudinal gradient in precipitation and elevation provides the ideal setup for exploring how spatially variable climate and topography can influence the geomorphic evolution of adjacent catchments.

Beyond the mountain front, a bajada of at least four generations of fan terraces extends into the Iglesia basin (Perucca & Martos, 2012). The development of these terraces lacks quantitative constraint, though elsewhere in the Andes, such cut and fill sequences have been linked to alternations between wet and dry periods on a variety of orbital timescales (Bekaddour et al., 2014; Litty et al., 2018; Norton et al., 2016; Siame et al., 1997; Steffen et al., 2009; Tofelde et al., 2017, 2019). We isolate three adjacent alluvial fans and focus on their modern rivers, which are currently incised ~2 m into a surface interpreted to be Holocene in age (Harries et al., 2018, 2019). The largest alluvial fan, fan 1, extends ~40 km into the centre of the basin, and is fed by two large catchments (2 and 3 in Figure 2). Fans 2 and 3, situated south and north of fan 1, respectively, extend ~25 km into the basin and are fed by catchments 1, and 4 and 5, respectively (Figure 2). The base level of these river systems is modulated by the Rodeo lake, which today is controlled by a man-made dam. The opening and closure of the basin through the Holocene, by episodic damming of the Jachal River, is evident from lake deposits preserved in the Jachal valley (Colombo et al., 2009).

3 | APPROACH

To explore how the glacial conditioning of a landscape influences connectivity, sediment export and the construction of stratigraphic records, we draw on three lines of evidence; (i) river network morphology and its relationship with spatial variability in bedrock lithology and precipitation, (ii) channel–hillslope morphology and (iii) alluvial fan gravel composition. Combined, these methodologies allow us to test a hypothesis that the lithological and climatic controls on landscape form are directly translated downstream into their sedimentary record. In this idealised case, we would expect source regions that are experiencing the greatest erosion rates to be over-represented in their sedimentary record (Litty et al., 2017). Where there is a deviation from this case, we can test the extent to which sediment storage and connectivity modulates sediment transfer through this postglacial landscape.

3.1 | Alluvial fan gravel analysis

As strong contrasts in rock resistance to abrasion could lead to significant, systematic downstream changes in relative abundance of clast types over distances of tens of kilometres (e.g. Attal & Lavé, 2006, 2009; Lavarini et al., 2018), we first test to what extent abrasion might have influenced the composition of sediment exported from each catchment. We do this by analysing the relationship between a clast's lithology and its size along the length of each fan. This is an ideal place to test an abrasion hypothesis as transport distances are in the order of tens of kilometres and the supply of fresh clasts from hillslopes is limited along the fans.

To characterise the composition of sediment exported to each of three alluvial fans, we recorded the lithology and size of a statistically significant number of gravels, $n \sim 200$ (Harries et al., 2018) at sites spaced at regular intervals along their fan length (Figure 2). On these dry riverbeds we also documented the proportion of the bed covered by sand. Sampling began ~3 km upstream of each bedrock canyon mouth and continued downstream at ~3 km intervals up to the fan's toe. These datasets were collected from the same localities as grain size datasets previously published in Harries et al. (2018, 2019). At each locality, approximately 50% of the clasts were sampled on the surface of a gravel bar and 50% from the channel, using the Wolman point counting technique, that is, clasts were selected randomly from within a predefined area of ~4 m^2 (Whittaker et al., 2010; Whittaker et al., 2011). The size of each clast was defined by its intermediate axis and was measured with a ruler. The lithology of each clast was categorised as intrusive, extrusive, sedimentary, metamorphic or quartzite. Whilst most clasts could easily be placed into these categories, the metamorphic overprint in some sedimentary clasts may have gone unrecognised, particularly for smaller pebbles; the metamorphic proportion of lithologies may therefore be underestimated.

We then isolated the lithologies that make up the coarse tail of the size distributions from those in the bulk of the distribution for all sites along the downstream length of each fan. The coarse tail was

defined as clasts coarser than 84% of the sample (>D_{84}) where the bulk of the distribution was defined as all clasts in the finer 84% of the distribution (<D_{84}). This allowed us to determine, firstly, if clasts derived from certain lithologies were systematically coarser grained than others and, secondly, if clasts of certain lithologies disappeared from the coarse tails with increasing distance from the fan apex. The latter would be expected if grains from a particular rock type reduced in size faster than others through abrasion. We subsequently evaluated the possibility that some bedrock lithologies preferentially weathered to grain sizes smaller than gravel on hillslopes. This can be the case if sediments spend a greater amount of time weathering on hillslopes or, given certain lithological traits (Riebe et al., 2015; Roda-Boluda et al., 2018). To analyse the potential for preferential sand production, we therefore observe the relative proportions of sand and gravel deposited on each fan in the context of their respective catchment traits, where we would expect catchments with steeper slopes and greater areal exposure of certain lithologies to produce relatively less sand.

3.2 | Catchment analysis

As the cordillera is currently tectonically stable, spatial variations in slope and channel steepness are expected to be dependent on the spatial variability in erosion rates, modulated by lithology and precipitation rates (D'Arcy & Whittaker, 2014; Hurst et al., 2013). We analyse the relationship between channel steepness and the spatial variability in bedrock lithology and precipitation rates across the cordillera to determine whether erosion, and therefore sediment production, is spatially variable. We then analyse the impact of glacial erosion on channel steepness and valley morphometry by testing the conceptual model outlined in Figure 1: main valleys influenced by glacial erosion are expected to be wider and less steep than those that are strictly fluvial, with tributaries notably steeper than their main valley (MacGregor et al., 2000). Finally, we use these observations to make predictions of what the composition of sediment ought to be given the erosional trends observed.

3.2.1 | Bedrock lithology

The lithology of bedrock exposed in each source catchment was derived from a geological map produced by the Servicio Geológico Minero Argentio, SegemAR. The units mapped (Figure 2) were not specific lithologies but formations or groups of rock units that were comparable to our pebble classification scheme, with the exception of quartzite and other metamorphosed lithologies which were found within the sedimentary Agua Negra Formation. These data were used in two ways: firstly, to quantify the relationship between channel steepness and bedrock lithology and, secondly, to compare the proportions of different pebble lithologies on the alluvial fans with their proportional areal exposure in each source catchment.

3.2.2 | Topographic analysis

We downloaded a 1 arc-second (approximately 30 m) resolution SRTM digital elevation model (DEM) for the study area from the USGS EarthExplorer database. Topographic analysis was performed using the LSDTopoTools algorithms (Mudd et al., 2014, 2018), detailed below. The topographic gradient was calculated by fitting a polynomial surface to a local window of elevations with a least-squares regression (Zevenbergen & Thorne, 1987), the details of which are outlined in Hurst et al. (2012).

We calculated the relative steepness of channels. Channels in headwaters tend to be steeper than channels further downstream, so some normalization is required to compare the steepness of channels at different points in the channel network (e.g. Wobus et al., 2006). Many authors have noted the power-law relationship between slope and discharge or its proxy drainage area (e.g. Morisawa, 1962), and this has been used to define a channel steepness index (e.g. (Wobus et al., 2006; Kirby & Whipple, 2012). The normalised channel steepness index, k_{sn}, at any point along the river network, i, can be defined as the product of local channel slope, S, and effective discharge, Q:

$$k_{sn} = Q^{\theta ref} S, \tag{1}$$

This requires the use of a reference concavity index, θref (Wobus et al., 2006; Kirby & Whipple, 2012).

Calculation of k_{sn} directly from Equation 1 is problematic because topographic slope can vary both due to reach-scale variations as well as errors in topographic data. As a result, some degree of smoothing is required (e.g. Wobus et al., 2006).

An alternative to using slopes is to use the elevation of the channel directly to calculate steepness through the derivation of a longitudinal coordinate that integrates discharge or drainage area, as first proposed by Royden et al. (2000).

The integrated coordinate can be illustrated by reference to an ideal channel where the elevation is perfectly defined by Equation (1). We can rearrange Equation (1) to solve for channel slope and, because slope is the derivative of elevation with respect to distance along the channel, we can solve this equation for elevation via integration (e.g. Royden et al., 2000). This results in an equation:

$$z(x) = z(x_b) + \left(\frac{k_s}{{Q_0}^{\theta}}\right)\int_{x_b}^{x}\left(\frac{Q_0}{Q(x)}\right)^{\theta} dx \tag{2}$$

where Q_0 is a reference discharge that ensures the integrand in Equation 2 is dimensionless and x_b is the distance of an arbitrary base level (e.g. Royden & Taylor Perron, 2013). We then define a coordinate, χ, which is of dimension length, as

$$\chi(x) = \int_{x_b}^{x}\left(\frac{Q_0}{Q(x\prime)}\right)^{\theta} dx' \tag{3}$$

We calculate χ for the channel network using Equation (3). We define $Q_0 = 1$ (for any chosen unit of discharge), so that the slope of

the channel profile in χ-elevation space (elevation is derived from the DEM) is equal to the channel steepness index. If the concavity index is fixed to the reference value, θ_{ref}, then the slope in χ-elevation space is equal to the normalised channel steepness index.

As we do not have direct measurements of discharge, it must be approximated. In this study, we do this in two ways. The first method, which is used in most studies, is to set discharge as proportional to drainage area (e.g. Kirby & Whipple, 2012; Wobus et al., 2006): $Q = k\,A$. We can then define the χ coordinate as

$$\chi_A(x) = \int_{x_b}^{x} \left(\frac{A_0}{A(x\prime)}\right)^{\theta} dx' \tag{4}$$

Where we use χ_A to denote that this coordinate is calculated using drainage area as a proxy for discharge.

In areas with strong precipitation gradients such as ours, however, discharge is not linearly proportional to drainage area. To overcome this limitation, we calculate the χ coordinate by accumulating precipitation (Babault et al., 2018):

$$\chi_P(x) = \int_{x_b}^{x} \left(\frac{P_0 A_0}{A(x\prime)P(x\prime)}\right)^{\theta} dx' \tag{5}$$

Where χ_P denotes the chi coordinate calculated using precipitation. The precipitation data used to compute Equation (5) over the cordillera is derived from a WorldClim dataset of maximum precipitation rate averaged over a 30 year period from 1970 to 2000 (Fick & Hijmans, 2017).

We denote the normalised steepness indices calculated using drainage area and precipitation as $k_{sn,A}$ and $k_{sn,P}$, respectively.

The use of a suitable concavity index, θ_{ref}, is necessary for calculating a meaningful normalised channel steepness index. In both steady-state and transient channel networks, the best fitting value of θ should result in tributaries being collinear with each other and the main stem channel in χ-elevation space (Royden & Taylor Perron, 2013). We quantify the most likely value of θ for each basin by minimising a disorder metric (Goren et al., 2014; Hergarten et al., 2016; Mudd et al., 2018) using the method of Mudd et al. (2018). We then calculate normalised channel steepness indices using the median value of θ across all the basins.

Comparison of normalised steepness indices calculated using the area-based approach to those calculated using the precipitation approach can be a challenge since these naturally take different values. We therefore calculate the z-score $Z_{k_{sn}}$ for each dataset and compare the two datasets using the difference between their z-scores. At each point i along the river network, the difference between the two z-scores is expressed as

$$\Delta Z_i = Z_{k_{sn,P,i}} - Z_{k_{sn,A,i}} = \left(\frac{k_{sn,P,i} - \bar{k_{sn,P}}}{\sigma_{kP}}\right) - \left(\frac{k_{sn,A,i} - \bar{k_{sn,A}}}{\sigma_{kA}}\right) \tag{6}$$

where $k_{sn,P,i}$ and $k_{sn,A,i}$ are the values of k_{sn} calculated at pixel i for $k_{sn,P}$ and $k_{sn,A}$, respectively, $\bar{k_{sn,P}}$ and $\bar{k_{sn,A}}$ are the mean values for each dataset, and σ_{kP} and σ_{kA} are their standard deviations.

The relationship between $k_{sn,P}$ and bedrock lithology is then analysed by grouping channels into the lithological formations they flow over and observing the distributions of z-scores of $k_{sn,P}$.

3.3 | Landscape connectivity and sediment storage

Based on the trends mapped out by channel steepness indices, and accounting for the spatial variation in lithology and precipitation, the gravel lithology datasets are used to determine whether the areas of the catchments that are expected to experience greater erosion contribute a larger proportion of sediment to their alluvial fans. In doing so, we test to what extent the sediment exported from these catchments represents a spatially integrated sample of upstream erosion. We then combine this analysis with morphometric mapping of hillslopes and channel deposits to determine whether sediment storage and landscape connectivity, both longitudinally and between hillslopes and channels, could have had a role in modulating sediment export from the cordillera.

Estimates of longitudinal connectivity would typically require detailed channel geometry measurements to formally calculate sediment transport capacities along the downstream length of the river networks. While we do not have these constraints, we can approximate the potential for sediment transport along the river network using the channel steepness indices, as bed slope and river discharge are dominant controls on sediment transport (Dietrich et al., 2003). Such an approximation of longitudinal connectivity utilising $k_{sn,P}$ is possible where slope is not dependent on the precipitation rate.

We explore hillslope–channel connectivity, using Google Earth to categorise catchment sediment deposits into three distinct groups based on morphological evidence for fluvial incision. We analyse all deposits with width > 100 m located within the main valley and > 5 km downstream of the headwaters, so to delimit the area of the catchment dominated by fluvial and not debris flow processes (Stock & Dietrich, 2003). Based on their morphological features, deposits are grouped as (1) floodplain deposits, (2) alluvial and colluvial fans that feed sediment directly to the main river channel, and (3) slope deposits and moraine that form terraces and ridges along valley sides. In combining these analyses, the role of climate in modulating connectivity and sediment export is explored within the context of the strong, along-strike precipitation gradient that prevails across the study area.

4 | RESULTS

The impact of past glaciation on the cordillera is evident from the cirque morphology of their headwaters, wide low-gradient valleys with steep tributaries, and the lateral and medial moraines that are preserved in their upper reaches (Figures 1, 2a). Today, small glaciers

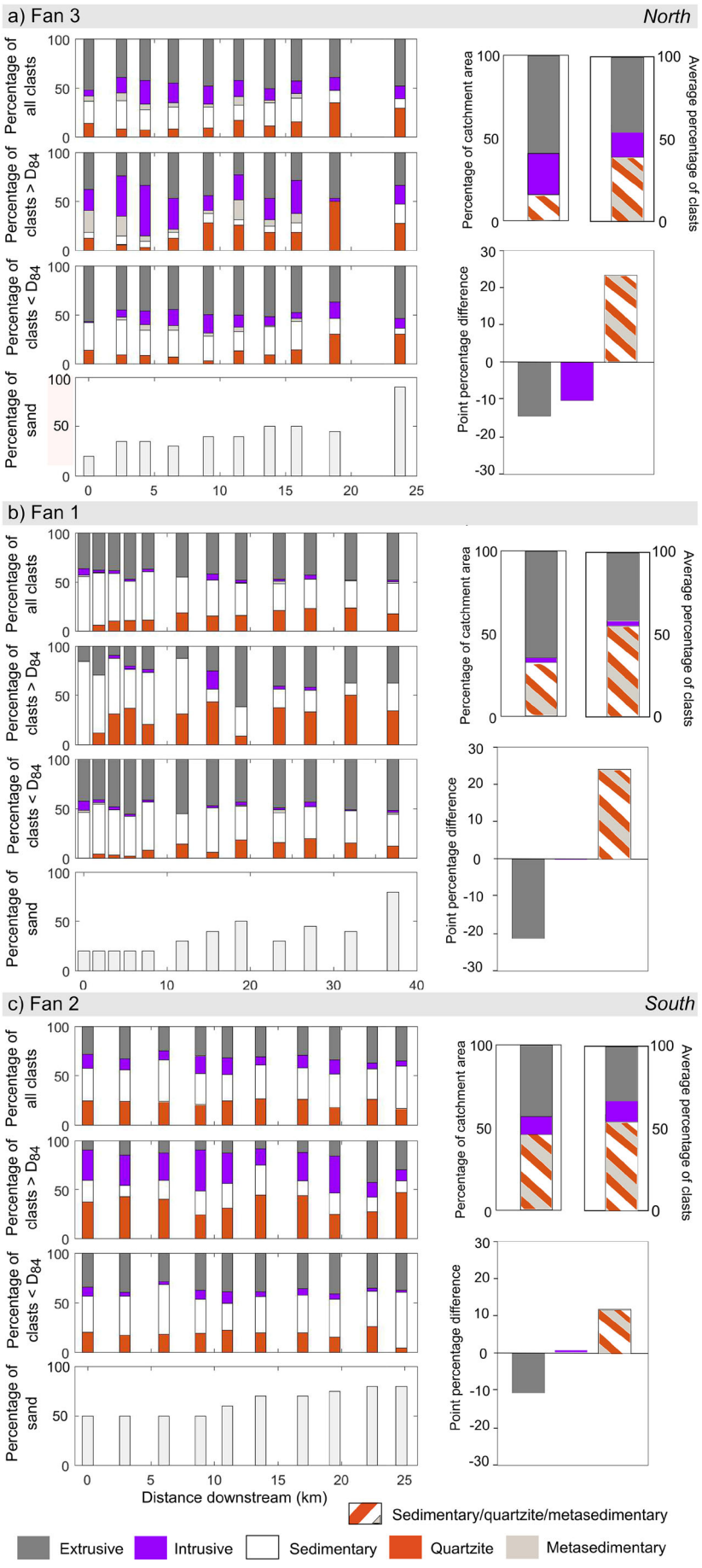

FIGURE 3 Riverbed gravel composition. For each fan, we present the proportions of different lithologies in the riverbed gravels deposited along the alluvial fans (left) and compare them with the proportions exposed as bedrock in their upstream catchments (right). On the left panels, the top plot presents the lithology of all clasts measured at sites along the length of the fan as classified in the field. The two middle plots present the lithology of clasts in the coarse tail of the size distribution (>D_{84}) and in the rest of the distribution (<D_{84}) at the same sites along the length of the fan. The bottom plot gives the percentage of sand estimated at each site. On the right, the proportions of gravel lithologies are averaged across the respective fan and compared to their source region; the bottom plot highlights the corresponding lithological bias

persist in north-facing headwaters, increasing in number and size to the south of the range where both peak elevations and precipitation rates are systematically higher. The shapes of the smaller catchments, 1, 4 and 5, are narrow and elongate such that tributaries are small and feed into a single main valley. The larger catchments 2 and 3 are wider where longer tributaries drain their north-facing slopes. The lithological composition of gravels sampled on each fan is first analysed to observe whether there are areas of these catchments that have preferentially supplied sediment to each fan over the Holocene.

4.1 | Alluvial fan sediments

Gravels make up to 80% of the riverbed surface area at the apex of fans 1 and 3, and 50% on fan 2, where the remaining area is composed of sediments that are finer than gravel. With distance downstream, the proportion of gravel on the bed surface decreases to 10%, 20% and 20% on fans 3, 1 and 2, respectively, over distances of 24, 37 and 25 km (Figure 3).

All major lithologies exposed in the catchments are represented on their respective fans. Along the downstream length of fans 2 and 3, we observe no systematic change in the abundance or size of different clast lithologies (Figure 3a, c). We do observe a stepwise decrease in the abundance of sedimentary clasts larger than D_{84} along the length of fan 1, from ~50% at the fan apex to ~30% at the fan toe. At ~12 km downstream this abrupt change coincides with a major confluence along the river (Figure 3b).

As there is no clear downstream trend and little variability, we can compare average lithological proportions in gravel across fans with the relative aerial contribution of each lithology in the contributing catchment (Figure 3). Extrusive lithologies make up 64% of fan 1's catchment area, while only 43% of riverbed gravels were extrusive clasts. Extrusive clasts are therefore under-represented in the riverbed gravels by a factor of 0.7 when compared with their source area exposure (Figure 3b). Up to 32% of the exposed bedrock is sedimentary or metasedimentary rock, including quartzite. On average, 39% of clasts were sedimentary, 15% were quartzite and 1% were metasedimentary, which, when grouped together (55%), gives an over-representation of sedimentary lithologies in the riverbed gravels by a factor 1.7. The limited exposure of intrusive bedrock in fan 1's catchment area is equally represented in their abundance in the riverbed gravels, ~3%.

In fan 2's catchment area, 42% of the bedrock is extrusive and, as with fan 1, the extrusive bedrock is under-represented in the riverbed gravels by a factor of 0.7, making up only 31% of riverbed gravels (Figure 3c). Sedimentary and metasedimentary bedrock, which makes up 46% of the catchment area, is slightly over-represented in the riverbed gravels by a factor of 1.2, as 34% of clasts are sedimentary and 23% are quartzite. On the other hand, intrusive lithologies are present in approximately the same proportion in the riverbed gravels as they are exposed in the catchment, 12%.

Fan 3 shows the least difference for extrusive bedrock, with an under-representation in its riverbed gravels by a factor of 0.75, where 59% of fan 3's catchment area is extrusive bedrock and 45% of clasts are extrusive lithologies (Figure 3). Intrusive lithologies make up only 15% of riverbed gravels and are also underrepresented by a factor of 0.5 with respect to their exposure in the source area. The remaining gravels are sedimentary or metasedimentary: 16% quartzite, 4% metasedimentary and 20% sedimentary, which together are over-represented by a factor of 2.6.

In all three catchment-fan systems, sedimentary lithologies from the lower cordillera are over-represented in the riverbed gravels, whereas extrusive lithologies from the upper cordillera are under-represented, compared to their source area exposure. The magnitude of this over-representation appears to increase northward across the cordillera. The proportion of sand deposited on the bed surface at the fan apex also seems to be greater in the south, where the sand proportion is ~30% higher on fan 2 than on the other two fans (Figure 3).

4.2 | Catchment trends

4.2.1 | Slope and channel steepness

A southward increase in range elevation is correlated with steeper slopes (Figure 4a). There is a systematic trend across all catchments for tributaries in the upper cordillera to be over-steepened relative to those in the lower cordillera (Figure 4b). Selecting a single concavity that satisfies the entire river network is therefore not possible: the distribution of best-fit values appears to be bimodal, producing large uncertainties that are evident in Figure 4d. Channel steepness is highly variable in the upper cordillera; however, a best fit is achieved with a concavity index of 0.45 ± 0.05. The lower cordillera, delineated as the area <10 km upstream of the catchment mouth, on the other hand, has a lower best fit concavity index of ~0.25 (Figure 4e).

As the best fit concavities and uncertainty ranges determined for $k_{sn,A}$ and $k_{sn,P}$ are the same, we use a median value of 0.47 to calculate both (Figure 4b). While recognising that the rainfall gradient does not appear to significantly influence profile concavities, the *z*-score distribution presented in Figure 4c does indicate that channels have a greater steepness (positive ΔZ_i) in the upper reaches when precipitation rates are accounted for.

In Figure 4e, we present chi-elevation profiles calculated using the best fit concavity derived for the lower cordillera, 0.25. Although this low value produces a weak relationship between slope and discharge at the catchment scale, it produces the best fit along the reaches of the river network that have the lowest steepness variability and are predominantly fluvial (as opposed to the glacially influenced channels in the upper part of the catchment). The low-gradient, wide main valleys with steep tributaries observed in the upper cordillera (Figure 4a, b) fit the profile predicted for alpine valleys that have been influenced by glaciation (Figure 1) (Anderson et al., 2006; MacGregor et al., 2009). The step change in relative channel steepness, characteristic of a knick-zone, is observed in all catchments at an elevation of 3,900 ± 100 m.

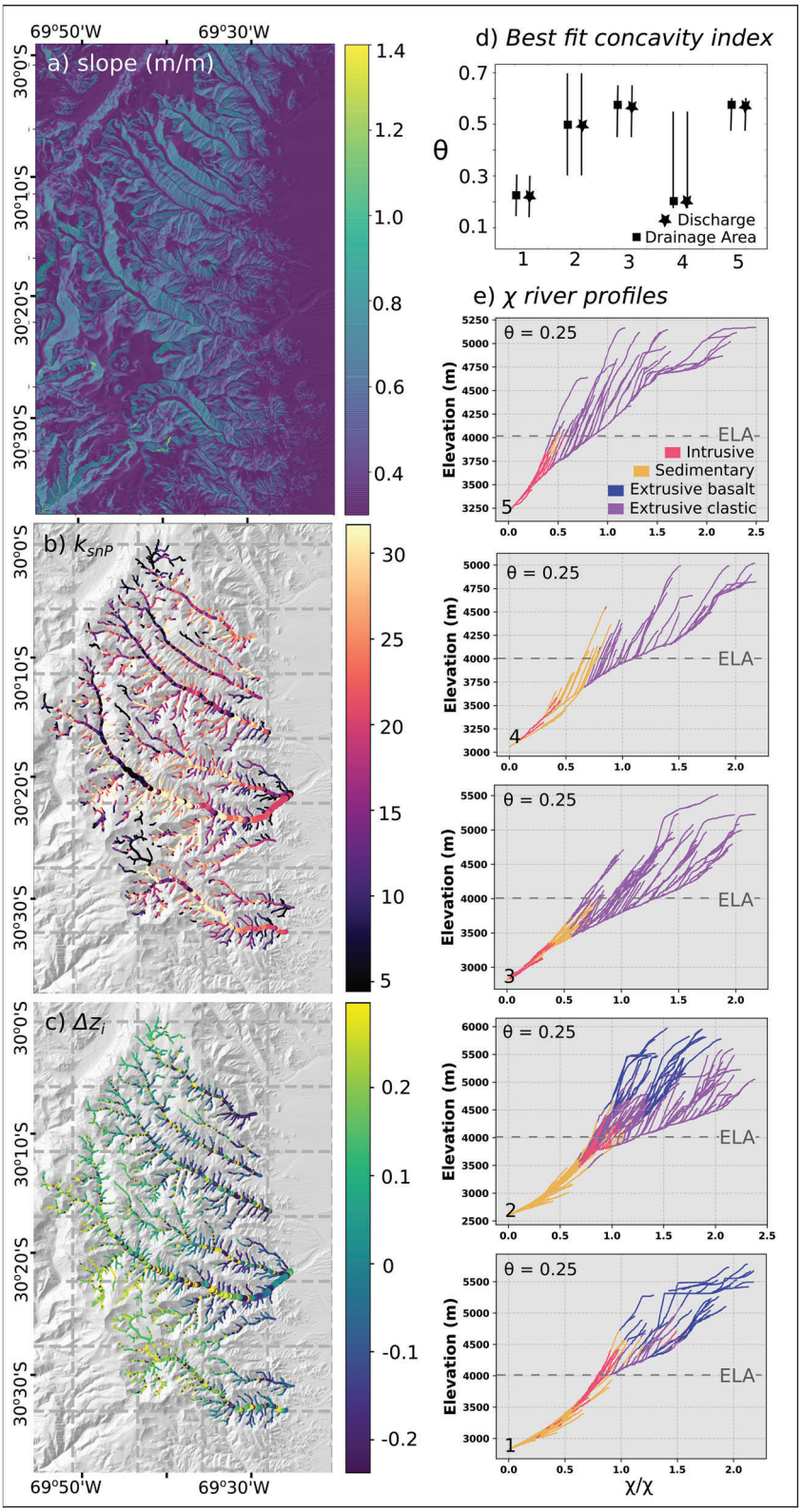

FIGURE 4 (a) Slope, (b) spatial distribution of $k_{sn,P}$, (c) ΔZ_i, the difference between the *z*-scores of $k_{sn,P}$ and $k_{sn,A}$ (Equation 6), d) best-fit concavity indices calculated using disorder metric for each catchment and (e) χ plots of all five catchments coloured according to lithology. Observe the disequilibrium between upstream and downstream reaches. With a concavity index of 0.25 (best fit for the lower cordillera), we observe tributaries upstream, above the Pleistocene ELA, that are variably over-steepened with respect to the main channel

4.2.2 | k_{sn} and bedrock lithology

The main river channels have a distinct pattern: the upper reaches have low k_{sn} values, whereas the lower reaches have high k_{sn} values (Figure 4b). These patterns in k_{sn} correlate spatially with distinct lithological units, highlighting a possible lithological control (Figure 4d). To assess this control, we analyse the relationship between channel steepness and lithology at the scale of the study area. Rivers draining the upper and lower reaches of the Frontal Cordillera erode extrusive volcaniclastic and sedimentary bedrock,

respectively. We observe, however, that there is no statistically significant difference in the distribution of k_{sn} between the river channels flowing over volcaniclastic and sedimentary bedrock (Figure 5, purple and yellow bars). Similarly, the distribution of k_{sn} in intrusive, granitic bedrock, which outcrops at the reach transition in catchments 1 and 2, is indistinguishable from the other rock types. A large variability in k_{sn} is observed for all rock types, with ranges of values overlapping significantly (Figure 5). These findings indicate there is no discernible correlation between bedrock lithology and channel steepness across the cordillera.

4.3 | Sediment dynamics

4.3.1 | Hillslope–channel morphology

The mapping of sediment deposits within the cordillera (Figure 6) shows that large hillslope and valley deposits are limited to the upper cordillera, in contrast with the deposits in the lower cordillera, which are fewer in number and smaller in area (beyond our mapping criteria). Valley-side terraces dominate the catchments that supply sediment to fans 1 and 3 (Figure 6). In some places, terrace scarps are more than 50 m in height. The upper valley of the largest catchments supplying fan 1 also have extensive floodplain deposits under which the toes of terraces are buried. In contrast, terraces are almost absent in the catchment supplying fan 2. There, alluvial and colluvial fans build out from the mouths of tributaries, feeding directly into the braided network of channels that fill the main valley. The majority of the sediment fans within the catchment have minimal breaks in slope at their toe. While these tributary fans lack toe scarps, they are incised in their headwaters and along their downstream length.

4.3.2 | Longitudinal connectivity

As we have demonstrated that channel steepness varies independently of precipitation rates and is not systematically affected by lithology, we can use $k_{sn,P}$ as a proxy for the sediment transport capacity (see methodology). We note that $k_{sn,P}$, and therefore the transport capacity, is lower in the main channel of the upper cordillera (Figure 4b), despite the elevated precipitation rates in these reaches (Figure 2). In comparing $k_{sn,P}$ and $k_{sn,A}$, we observe that the steepness index is higher in the upper cordillera of the southern catchments when the spatial variability in precipitation rate is accounted for (higher and lower ΔZ_i, respectively). The steepness indices of the northern catchments, however, are comparable between methods.

5 | DISCUSSION

5.1 | Sediment sourcing

The composition of gravels on three alluvial fans in the Iglesia basin are dominated by lithologies exposed in the lower reaches of their source areas. While the greater transport distance of upper cordillera clasts or contrasts in rock resistance to abrasion have been evoked to explain this trend in other river systems (e.g. Attal & Lavé, 2006, 2009; Dingle et al., 2017; Lavarini et al., 2018), here we observe that all major lithologies are represented in each fan, with no evidence of systematic downstream changes in the relative abundance of clasts over distances of tens of kilometres (Harries et al., 2019). These observations, along with the fact that all major lithologies are represented in each fan, suggests abrasion cannot be a major control on sediment composition in this study area. Where we do observe an abrupt compositional change along the length of the largest fan, the distance at which this occurs corresponds with a major confluence, as such, we attribute the compositional change to the mixing and dilution of sediment sources on the fan and not abrasion.

We acknowledge that we cannot rule out the disappearance of particularly weak sub-lithologies through abrasion within a given lithological category before they reach the fan (e.g. some of the slightly metamorphosed mudstones and sandstones from the Agua Negra formation within the sedimentary category). However, we consider that preferential disintegration of upper cordillera bedrock to

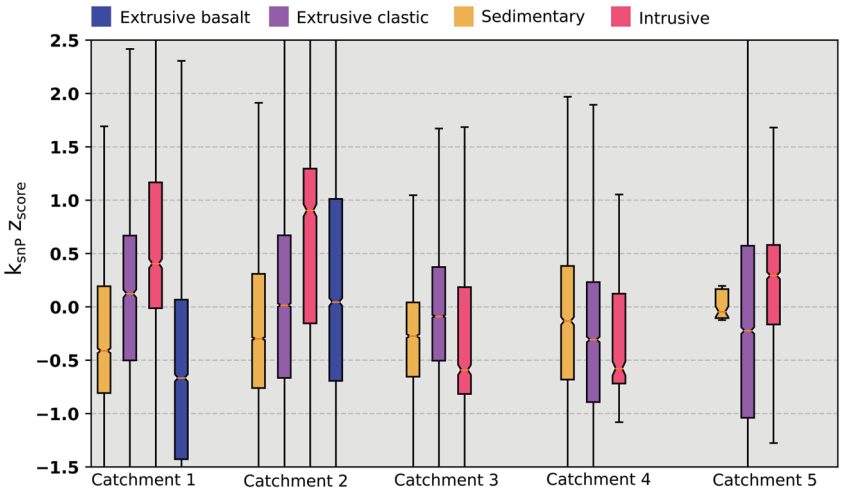

FIGURE 5 Distribution of z-score for $k_{sn,P}$ within each bedrock lithology for each catchment

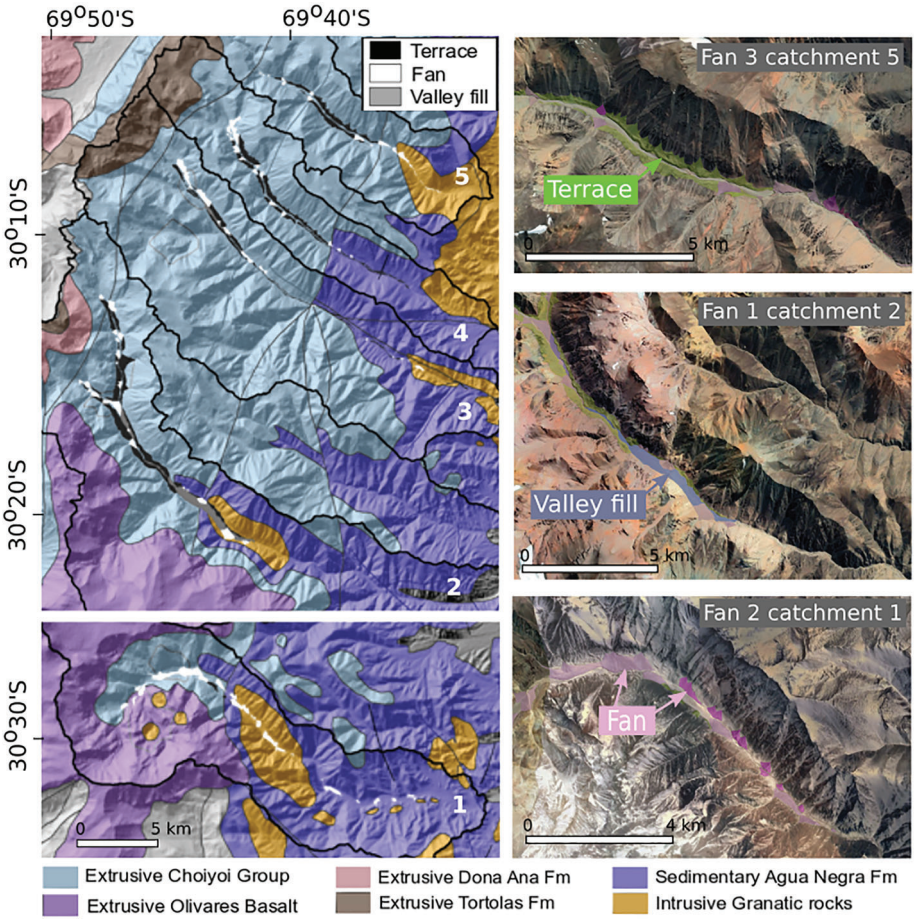

FIGURE 6 (a–f) Mapping of sediment deposits within the Argentine cordillera. (c–e) Google Earth images illustrating the different types of deposits. Terrace deposits dominate the catchments that feed fans 1 and 3 (a, c, d), whereas alluvial-colluvial fans are conspicuous in the catchment that feeds fan 2 (b, e)

sand rather than gravel cannot explain the under-representation of volcanics in the fans. If this were the case, the expectation would be that the catchment with the shallowest slopes and largest areal exposure of the underrepresented bedrock would have produced the largest relative contribution of sand. However, we observe the opposite: The catchment of fan 2, which has both the smallest areal exposure of volcani-clastic bedrock and the steepest slopes is exporting twice as much sand and a greater proportion of volcani-clastic gravels compared with the other catchments.

In the absence of a clear abrasion or weathering control on sediment composition, we explore alternative hypotheses drawing on the following observations: (1) channel steepness varies both across the cordillera and within the individual catchments and (2) sedimentary deposits have accumulated where channel steepness is low.

The first alternative hypothesis to test to account for an over-representation of sedimentary clasts is that bedrock erosion rates are higher in the sedimentary units of the lower cordillera. As the distributions of channel steepness, $k_{sn,P}$ are highly variable across all lithological classes, it suggests that bedrock lithology does not determine erosion rate (z scores, Figure 5). Indeed, the mapping of deposits within each catchment (Figure 2, 6) combined with the topographic analysis (Figures 1, 2, 4) reveal that erosion and sediment production may be enhanced in the upper cordillera. Consequently, we reject the hypothesis that an over-representation of sedimentary clasts in this setting is due to a higher rate of sedimentary bedrock erosion. An enhanced upper cordillera erosion signal is not translated downstream to the alluvial fans, even under the assumption of uniform catchment-wide erosion rates, as shown by the systematic deficit in extrusive clasts (Figure 3). Consequently, the attenuation of the upper cordillera sediment signal can only be explained by storage of sediment upstream of the corresponding alluvial fan.

Mapping highlights areas of sediment storage that are unique to the upper cordillera, in the form of terraces, alluvial/colluvial fans and valley fills. The upper cordillera, where storage regions prevail, has a distinct valley morphometry compared with the lower cordillera, with main valley thalwegs that are wider, less steep, and tributaries that are steeper than the main valley. These observations fit with a conceptual model for glacial erosion in the upper cordillera (MacGregor et al., 2009) (Figure 1), which is further supported by the presence of cirques, moraine and ice and rock glaciers in the headwaters of these catchments. While highly variable steepness in the upper cordillera can be well explained by glacial carving, the low concavity of the lower cordillera is unexpected, though could well be attributed to the role of glacial sediment in formerly blanketing these reaches or downstream changes in channel width. The potential for valleys to both produce and store sediment following glaciation has long been recognised (Ballantyne, 2002). We find that the main transition between upstream reaches with low steepness indices and

downstream reaches with high steepness indices occurs at an elevation of ~3,800 m on all main river profiles, which approximates the Pleistocene ELA previously reported for the dry Andes, ~4,000 m (Clapperton, 1994). While there are no terminal moraines to verify the limits of past glaciation in these catchments, we interpret the transition between upstream segments of low k_{sn} and downstream segments of high k_{sn} as a marker of the downstream extent of glacial erosion, cumulated over several Quaternary glaciations (Korup & Montgomery, 2008; Montgomery & Korup, 2011).

5.2 | Climate control on sediment export

An inverse correlation between the spatial distribution of channel steepness, which is lower in the upper cordillera (Figure 4b), and precipitation rate, which is higher (Figure 2), suggests that slope could be a function of precipitation pattern (D'Arcy & Whittaker, 2014). The morphology of the upper cordillera, however, indicates that glacial erosion, and not precipitation rate, has been the dominant control on channel gradient here (Anderson et al., 2006; MacGregor et al., 2009). While accounting for the spatial distribution of precipitation rates in calculations of k_{sn} results in higher channel steepness indices (Figure 4c), this increasing effect does not compensate for the low channel gradients in this region. Interpreting $k_{sn,P}$ as a proxy for the sediment transport capacity along the river network, we observe that there is a low potential for sediment transport, where $k_{sn,P}$ is lowest, in the upper cordillera, despite the enhanced precipitation focused on this region. The upper cordillera may be interpreted as being, to some extent, decoupled from the lower cordillera by its low gradient reaches. Such a decoupling is further evidenced by the presence of a knick-zone between the upper and lower cordillera.

While the decoupling of upstream reaches from those downstream can explain the under-representation of gravel sourced from upper cordillera bedrock on the fans, we observe that both the degree to which the upper cordillera is under-represented on the fans and the hillslope–channel morphology varies between the three catchment-fan systems. We first observe that the largest catchments feeding fan 1 has the lowest $k_{sn,P}$, and therefore the lowest potential for sediment mobilisation, in its upper cordillera (Figure 4). These low-mobility reaches comprise large valley fills and terraces, which are indeed indicative of sediment storage (Figure 6). Correspondingly, fan 1 has the lowest representation of upper cordillera clasts in its gravels. We observe discrete differences between the two catchment-fan systems of similar size, fans 2 and 3. Fan 3's contributing catchments have a higher $k_{sn,P}$ in their upper reaches than the other catchments and therefore a higher potential for sediment mobilisation, yet the presence of extensive terraces in their upper cordillera indicates a high potential for sediment storage (Figure 6). Furthermore, the alluvial gravels of fan 3 are dominated by sediments sourced from the lower cordillera. Conversely, the upper reaches of the catchment feeding fan 2 has a lower $k_{sn,P}$ and therefore lower potential for mobilisation, yet terraces are few in these reaches, and clasts from the upper cordillera are better represented on fan 2's fan (Figure 6).

The transfer of upper cordillera clasts downstream does not therefore appear to be directly linked to channel gradient and discharge, described more generally as the longitudinal connectivity between the upstream and downstream reaches. Discrete differences in how sediment is being stored within the different catchments are recognised, which elude to hillslope–channel connectivity being an important modulator of long-term sediment export at a basin scale.

5.2.1 | Climate and hillslope–channel connectivity

The catchment sourcing fan 2 is unique in having few terraces and an abundance of large colluvial/alluvial fans that feed sediment from tributaries into the braided river channels of the main valley (Figure 6). Fans can act as buffers of hillslope–channel connectivity when aggrading under high sediment supply conditions (Bowman, 2018; Mather et al., 2017). On the other hand, they can be effective hillslope–channel couplers if the sediment supply from upstream is limited and incision is focused on the fan itself, thereby promoting the remobilisation of previously stored sediment (Bowman, 2018; Mather et al., 2017). The majority of the alluvial/colluvial fans within the catchment have minimal or concave breaks in slope at their toe, indicative of fan aggradation in the absence of main valley incision that would otherwise produce scarps. While this suggests some level of hillslope–channel buffering, the alluvial-type fans in this catchment are currently incised in their upper reaches and in some cases, along their length. Such a top-down incisional trend is an indication of at least partial coupling between the tributaries and the main channel (Mather et al., 2017).

In contrast, there is an abundance of terraces with large scarps in the catchments feeding fans 1 and 3. While main valley incision in fluvial settings is generally thought to promote hillslope–channel coupling (Attal et al., 2015; Whittaker et al., 2010), the creation of large terraces here suggest that valley incision has had an adverse effect on coupling in these widened, post-glacial valleys. Such large terraces not only store older hillslope sediments but also limit younger hillslope sediments in reaching the active channel. The evacuation of such terraced sediments ought to be dependent on the ability of the main channel to migrate laterally across the widened valley (Blum et al., 2013; Carretier et al., 2020).

Our gravel data confirm that the catchments that show clear evidence of main valley incision, that is, have large terraces, export less sediment from their upper cordillera. Conversely, the catchment that has morphological evidence for main valley aggradation and headwater incision focused in its tributary fans is exporting a greater proportion of upper cordillera clasts. This trend is reflected in the proportions of sand exported to the fans, which is over twice as high on the fan dominated by top-down tributary fan incision, fan 2. We therefore infer that a greater degree of connectivity between hillslopes and channels, which results in greater sediment export, is achieved here when sediment is efficiently transferred from tributary fans to main valleys, without main valley incision.

Given that the incision and aggradation dynamics of these sediment systems are dependent on the ratios of sediment and water fluxes delivered to them (Tofelde et al., 2019), we can explore these relationships in the context of spatially variable precipitation (Figure 7). Where both precipitation rates and the abundance of glaciers are highest in the south, we observe the highest degree of hillslope–channel connectivity and the greatest relative abundance of upper cordillera sediment deposited downstream. We hypothesise that higher precipitation rates in the headwaters of the cordillera can promote the transfer of sediment from tributaries to the main valleys (Meigs et al., 2006). In the main valley, an ample supply of sediment limits river incision, thereby ensuring greater connectivity between hillslopes, tributaries and the main channel. This behaviour is observed in numerical models of drainage basin evolution where increased runoff intensities initiate expansion of the channel network and aggradation along the main channel while sediment supply remains high (Tucker & Slingerland, 1997). Conversely, when precipitation rates are lower, the potential for sediment storage in tributaries ought to be greater. We suggest that such upstream storage limits sediment supply to the main valley and promotes main river incision and terrace formation (Tofelde et al., 2019). Consequently, we find that the geomorphic response of adjacent river networks to a relatively subtle spatial variability in climate can be markedly different. This has important implications for understanding the evolution of threshold-dominated landscapes such as the arid Andes. Building on previous work investigating sediment recycling dynamics on the Iglesia basin fans (Harries et al., 2018), we can also reconcile evidence for greater catchment connectivity being associated with a lesser degree of fan recycling, akin to the findings of Malatesta et al. (2018).

5.3 | Controls on glacial imprint and connectivity

The rate of bedrock erosion by warm-based glaciers, which co-varies with their downstream length, is known to be controlled by both climate and catchment morphology (Brocklehurst & Whipple, 2004; Cook et al., 2020; Koppes et al., 2015). While a quantitative relationship between glacial erosion and channel steepness does not yet exist, relative differences in channel steepness across the upper cordillera ought to preserve information about the wider climatic and lithologic controls on glacial erosion and have implications for the post-glacial recovery of the landscape (Prasicek et al., 2020). This requires an assumption that the relatively uniform steepness indices of the lower cordillera are roughly representative of a pre-glacial river profile, such that the reduction in channel steepness can be interpreted as a function of erosional efficiency. Additionally, it assumes that the change in channel steepness at the approximate altitude of the Pleistocene ELA marks the downstream extent of glacial erosion. Accordingly, a key observation is that channel steepness in the upper cordillera varies with catchment size and range elevation (Figure 2). We find that catchments with a greater area above the elevation of the approximate Pleistocene ELA have a lower average channel steepness in the main valley of their upper cordillera. The maintenance of relief in catchments with a larger glacial imprint, here recognised as the degree to which main valleys have been widened and lowered, suggests however that glacial erosion has not had a dominant role in limiting the relief of the mountain range (Brozović et al., 1997; Egholm et al., 2009; Pedersen et al., 2010). The fingerprint of glaciation in these catchments must therefore have been modulated by another factor controlling relief (Brocklehurst & Whipple, 2004).

While the steepness of channels draining different bedrock lithologies varies between catchments (Figure 5), the distribution of relief across the cordillera does correlate with outcrops of hard bedrock, specifically the exposure of relatively young basalts in the southern cordillera, which create a plateau at high elevation. Given that the width of the mountain range does not vary along strike, the observed increase in hillslope gradient with range elevation suggests that the increased bedrock resistance to erosion in the southern catchments could contribute to the along strike variability in elevation

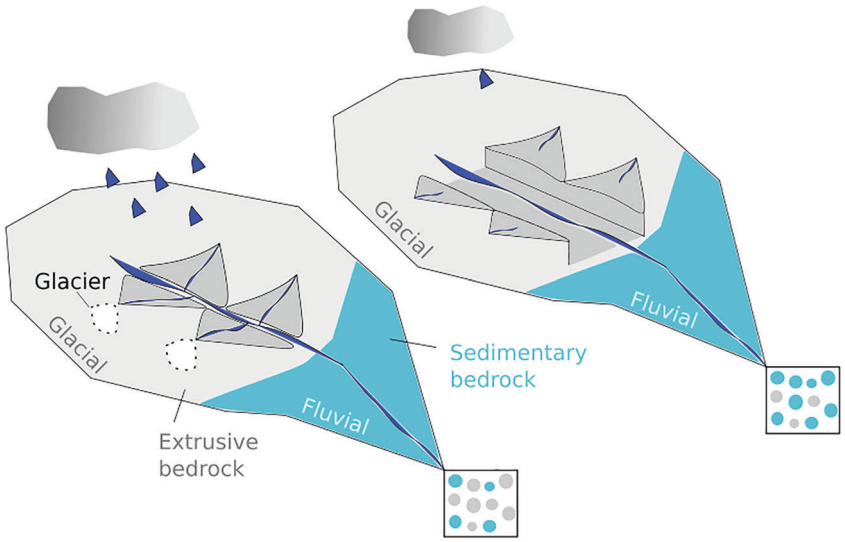

FIGURE 7 Conceptual model: The catchment with the highest precipitation rate has greater hillslope–channel connectivity, promoted by the delivery of sediment from its hillslopes and tributaries to its main valley. This promotes both main valley aggradation and sediment export from the upper reaches downstream, to its alluvial fan. The catchments with lower precipitation rates have poor hillslope–channel connectivity due to the limited delivery of sediment from their headwaters. This triggers main valley incision and limits sediment export from the upper cordillera

(Stutenbecker et al., 2016). As both elevation and its co-variant precipitation strongly influence the elevation of the ELA, there is evidence to suggest that the fingerprint of glaciation is modulated by the erodibility of the bedrock sequence. More locally, outcrops of hard granite, which coincide with the transitions from fluvially to glacially influenced reaches in some catchments, may also play a role in modulating the rate of bedrock incision and the re-equilibration of the postglacial landscape upstream.

The maintenance of elevation in these catchments ensures that they also experience higher precipitation rates in post glacial periods, which promotes both continued alpine glacial activity and the delivery of a greater water flux to the river network. This greater discharge may support the evacuation of sediment from tributaries to the main valley, as inferred from fan 2's catchment morphology. In this way, the wider lithological controls on topography may also precondition the effectiveness of river networks in evacuating their long-term sediment supply and the translation of erosion signals to their basin sedimentary record.

5.4 | Wider implications

Numerous models of river network evolution assume that the size and volume of sediment exported from a catchment is a function of slope, drainage area and some consideration of how sediment discharge diverges or reduces in size with increasing transport distance (Gasparini et al., 2004; Hobley et al., 2011). A downstream reduction in coarse, gravel supply is most readily considered a function of clast abrasion during transport (Dingle et al., 2017; Lukens et al., 2016; Wickert & Schildgen, 2019). This study, based in an area with no significant contrasts in abrasion rates between the different lithologies exposed, demonstrates that erosion signals are also heavily modulated by the degree of connectivity between hillslopes and river channels. As we demonstrate that connectivity and sediment export from catchments is sensitive to climate through its influence on sediment delivery to the river network, this has important implications for our understanding of how climate influences the evolution of river networks (Gasparini et al., 2007; Hodge et al., 2011), particularly following glacial perturbation.

While we have demonstrated qualitatively that sediment storage and release is a critical modulator of sediment flux from these mountain catchments, there is an outstanding question regarding the timescales over which these processes operate. In these glacial-widened valleys, river terraces have been abandoned as the main river has incised, and in a number of catchments, terrace deposits have been sealed by modern valley-fill sediments, indicating long-term (>10^3 years) sediment storage. The presence of at least four large alluvial terraces on the Iglesia basin fans (Harries et al., 2019), however, provides evidence for a step-wise increase in sediment export once deposits are mobilised. These findings highlight the potential for a disproportionate increase in sediment export under future climate scenarios if sediments previously stored can be rapidly mobilised downstream (Clapp et al., 2000). As the mobilisation of sediment stores in mountain regions impacts the morphology of rivers from mountain front to coast, an understanding of their sensitivity to climatic change is essential for predicting future societal impacts.

Finally, given our primary observation that source areas along glaciated reaches are under-represented in the sediments deposited downstream of the mountain front (Blöthe & Korup, 2013), we highlight a potential bias in the application of cosmogenic radionuclide methods and thermochronology to sand and, more recently, riverbed gravels, to reconstructing erosion or exhumation in mountain catchments (Lavarini et al., 2018; Lukens et al., 2020). Our results underline the fact that a clear understanding of source area dynamics is critical for constraining the sensitivity of the sedimentary record to external forcing.

6 | CONCLUSIONS

Sediment deposited on three alluvial fans in the Andes is preferentially sourced from the lower reaches of their mountain catchments. By examining the relationship between clast lithology and size, we demonstrate that this lithological bias cannot be explained by abrasion. Similarly, through an analysis of the steepness of longitudinal river profiles, we infer that the bias cannot be explained by the preferential erosion of the lower cordillera bedrock. Instead we conclude that the differences between the abundances of lithological classes on the alluvial fans and the distribution of bedrock types in the source catchments is explained by sediment storage in the upper cordillera. The segmentation of the river profiles fits well with a glacial erosion hypothesis where main channels in the upper cordillera have a lower gradient and their tributaries are systematically steeper. Erosion focused in the upper cordillera is not communicated downstream to the alluvial fans, and it is likely that this sediment is being stored upstream in over-deepened and over-widened glacial valleys. This hypothesis is corroborated by the observation that sediment storage is largely limited to the upper cordillera.

Drawing on both sedimentological and geomorphological datasets, we highlight a correlation between the composition of alluvial gravels and the dominance of two different types of sediment storage within the cordillera. Upper cordillera clasts are most under-represented downstream of catchments dominated by terrace deposits. The sediments deposited downstream of a catchment dominated by alluvial–colluvial fans are more enriched with upper cordillera clasts and sand. We therefore recognise hillslope–channel connectivity as a critical modulator of sediment export from these Andean catchments. By placing these trends within the context of an along-strike variation in topographic elevation and its co-variant precipitation, the importance of precipitation in promoting hillslope–channel connectivity and sediment export is recognised. As a result, we highlight the importance of considering the geomorphological evolution of source areas when reconstructing tectonic and climatic histories from stratigraphy.

ACKNOWLEDGEMENTS

R.M.H. was funded by NERC E3 DTP studentship NE/L002588/1 and The School of Geosciences at The University of Edinburgh, with further support from the Research Center for Integrated Disaster Risk Management (CIGIDEN) ANID/FONDAP/15110017. B.G. was funded by European Union initial training grant 674899 – SUBITOP. The authors wish to thank Fritz Schlunegger and an anonymous reviewer for their detailed comments that helped to improve the manuscript. We declare no conflicts of interest.

DATA AVAILABILITY STATEMENT

The data published here are available from the corresponding author upon reasonable request.

ORCID

Rebekah M. Harries https://orcid.org/0000-0002-6855-2122
Boris Gailleton https://orcid.org/0000-0001-6518-4304
Linda A. Kirstein https://orcid.org/0000-0001-5496-4081
Mikael Attal https://orcid.org/0000-0001-8639-6090
Simon M. Mudd https://orcid.org/0000-0002-1357-8501

REFERENCES

Allen, P.A. (2008) From landscapes into geological history. *Nature*, 451 (7176), 274–276. https://doi.org/10.1038/nature06586

Amidon, W.H., Burbank, D.W., & Gehrels, G.E. (2005a) Construction of detrital mineral populations: Insights from mixing of U-Pb zircon ages in Himalayan rivers. *Basin Research*, 17(4), 463–485. https://doi.org/10.1111/j.1365-2117.2005.00279.x

Amidon, W.H., Burbank, D.W., & Gehrels, G.E. (2005b) U-Pb zircon ages as a sediment mixing tracer in the Nepal Himalaya. *Earth and Planetary Science Letters*, 235(1-2), 244–260. https://doi.org/10.1016/j.epsl.2005.03.019

Anderson, R.S., Molnar, P. & Kessler, M.A. (2006) Features of glacial valley profiles simply explained. *Journal of Geophysical Research - Earth Surface*, 111(F1). https://doi.org/10.1029/2005JF000344

Attal, M. & Lavé, J. (2006) Changes of bedload characteristics along the Marsyandi River (Central Nepal): Implications for understanding hillslope sediment supply, sediment load evolution along fluvial networks, and denudation in active orogenic belts. *Special Paper of the Geological Society of America*, 398, 143–171. https://doi.org/10.1130/2006.2398(09)

Attal, M. & Lavé, J. (2009) Pebble abrasion during fluvial transport: Experimental results and implications for the evolution of the sediment load along rivers. *Journal of Geophysical Research - Earth Surface*, 114(F4). https://doi.org/10.1029/2009JF001328

Attal, M., Mudd, S.M., Hurst, M.D., Weinman, B., Yoo, K. & Naylor, M. (2015) Impact of change in erosion rate and landscape steepness on hillslope and fluvial sediments grain size in the Feather River basin (Sierra Nevada, California). *Earth Surface Dynamics*, 3(1), 201–222. https://doi.org/10.5194/esurf-3-201-2015

Babault, J., Viaplana-Muzas, M., Legrand, X., van den Driessche, J., González-Quijano, M. & Mudd, S.M. (2018) Source-to-sink constraints on tectonic and sedimentary evolution of the western central range and Cenderawasih Bay (Indonesia). *Journal of Asia Earth Sciences*, 156, 265–287. https://doi.org/10.1016/j.jseaes.2018.02.004

Ballantyne, C.K. (2002) A general model of paraglacial landscape response. *The Holocene*, 12(3), 371–376. https://doi.org/10.1191/0959683602hl553fa

Baynes, E.R.C., Lague, D., Steer, P., Bonnet, S. & Illien, L. (2020) Sediment flux-driven channel geometry adjustment of bedrock and mixed gravel–bedrock rivers. *Earth Surface Processes and Landforms*, 45(14), 3714–3731. https://doi.org/10.1002/esp.4996

Bekaddour, T., Schlunegger, F., Vogel, H., Delunel, R., Norton, K.P., Akçar, N. *et al.* (2014) Paleo erosion rates and climate shifts recorded by quaternary cut-and-fill sequences in the Pisco valley, Central Peru. *Earth and Planetary Science Letters*, 390, 103–115. https://doi.org/10.1016/j.epsl.2013.12.048

von Blanckenburg, F. (2005) The control mechanisms of erosion and weathering at basin scale from cosmogenic nuclides in river sediment. *Earth and Planetary Science Letters*, 237(3-4), 462–479. https://doi.org/10.1016/j.epsl.2005.06.030

Blöthe, J.H. & Korup, O. (2013) Millennial lag times in the Himalayan sediment routing system. *Earth and Planetary Science Letters*, 382, 38–46. https://doi.org/10.1016/j.epsl.2013.08.044

Blum, M., Martin, J., Milliken, K. & Garvin, M. (2013) Paleovalley systems: Insights from Quaternary analogs and experiments. *Earth-Science Reviews*, 116, 128–169. https://doi.org/10.1016/j.earscirev.2012.09.003

Bowman, D. (2018) *Principles of alluvial fan morphology*. Netherlands: Springer. https://doi.org/10.1007/978-94-024-1558-2

Brardinoni, F., Picotti, V., Maraio, S., Bruno, P.P., Cucato, M., Morelli, C. *et al.* (2018) Postglacial evolution of a formerly glaciated valley: Reconstructing sediment supply, fan building, and confluence effects at the millennial time scale. *Bulletin Geological Society of America*, 130(9-10), 1457–1473. https://doi.org/10.1130/B31924.1

Brocklehurst, S.H. & Whipple, K.X. (2002) Glacial erosion and relief production in the eastern Sierra Nevada, California. *Geomorphology*, 42(1-2), 1–24. https://doi.org/10.1016/S0169-555X(01)00069-1

Brocklehurst, S.H. & Whipple, K.X. (2004) Hypsometry of glaciated landscapes. *Earth Surface Processes and Landforms*, 29(7), 907–926. https://doi.org/10.1002/esp.1083

Brozović, N., Burbank, D.W. & Meigs, A.J. (1997) Climatic limits on landscape development in the northwestern Himalaya. *Science*, 276(5312), 571–574. https://doi.org/10.1126/science.276.5312.571

Carretier, S., Guerit, L., Harries, R., Regard, V., Maffre, P. & Bonnet, S. (2020) The distribution of sediment residence times at the foot of mountains and its implications for proxies recorded in sedimentary basins. *Earth and Planetary Science Letters*, 546, 116448. https://doi.org/10.1016/j.epsl.2020.116448

Castelltort, S. & Van Den Driessche, J. (2003) How plausible are high-frequency sediment supply-driven cycles in the stratigraphic record? *Sedimentary Geology*, 157(1-2), 3–13. https://doi.org/10.1016/S0037-0738(03)00066-6

Church, M. & Ryder, J.M. (1972) Paraglacial sedimentation: A consideration of fluvial processes conditioned by glaciation. *Bulletin Geological Society of America*, 83(10), 3059. https://doi.org/10.1130/0016-7606(1972)83[3059:PSACOF]2.0.CO;2

Clapp, E.M., Bierman, P.R., Schick, A.P., Lekach, J., Enzel, Y. & Caffee, M. (2000) Sediment yield exceeds sediment production in arid region drainage basins. *Geology*, 28(11), 995. https://doi.org/10.1130/0091-7613(2000)28<995:SYESPI>2.0.CO;2

Clapperton, C.M. (1994) The quaternary glaciation of Chile. *Revista Chilena de Historia Natural*, 67(4), 369–383.

Colombo, F., Busquets, P., Sole de Porta, N., Limarino, C.O., Heredia, N., Rodriguez-Fernandez, L.R. *et al.* (2009) Holocene intramontane lake development: A new model in the Jáchal River valley, Andean Precordillera, San Juan, Argentina. *Journal of South American Earth Sciences*, 28(3), 229–238. https://doi.org/10.1016/j.jsames.2009.03.002

Cook, S.J., Swift, D.A., Kirkbride, M.P., Knight, P.G. & Waller, R.I. (2020) The empirical basis for modelling glacial erosion rates. *Nature Communications*, 11(1), 759. https://doi.org/10.1038/s41467-020-14583-8

D'Arcy, M. & Whittaker, A.C. (2014) Geomorphic constraints on landscape sensitivity to climate in tectonically active areas. *Geomorphology*, 204, 366–381. https://doi.org/10.1016/j.geomorph.2013.08.019

D'Arcy, M., Schildgen, T.F., Strecker, M.R., Wittmann, H., Duesing, W., Mey, J. *et al.* (2019) Timing of past glaciation at the sierra de Aconquija, northwestern Argentina, and throughout the Central Andes. *Quaternary Science Reviews*, 204, 37–57. https://doi.org/10.1016/j.quascirev.2018.11.022

Delunel, R., Schlunegger, F., Valla, P.G., Dixon, J., Glotzbach, C., Hippe, K. *et al.* (2020) Late-Pleistocene catchment-wide denudation patterns across the European Alps. *Earth-Science Reviews*, 211, 103407. https://doi.org/10.1016/j.earscirev.2020.103407

Dietrich, W.E., Bellugi, D., Heimsath, A.M., Roering, J.J., Sklar, L. & Stock, J.D. (2003) Geomorphic transport laws for predicting landscape form and dynamics. *Geophysical Monograph Series*, 135, 103–132. https://doi.org/10.1029/135GM09

Dingle, E.H., Attal, M. & Sinclair, H.D. (2017) Abrasion-set limits on Himalayan gravel flux. *Nature*, 544(7651), 471–474. https://doi.org/10.1038/nature22039

Egholm, D.L., Nielsen, S.B., Pedersen, V.K. & Lesemann, J.E. (2009) Glacial effects limiting mountain height. *Nature*, 460(7257), 884–887. https://doi.org/10.1038/nature08263

Fick, S.E. & Hijmans, R.J. (2017) WorldClim 2: New 1-km spatial resolution climate surfaces for global land areas. *International Journal of Climatology*, 37(12), 4302–4315. https://doi.org/10.1002/joc.5086

Gasparini, N.M., Tucker, G.E. & Bras, R.L. (2004) Network-scale dynamics of grain-size sorting: Implications for downstream fining, stream-profile concavity, and drainage basin morphology. *Earth Surface Processes and Landforms*, 29(4), 401–421. https://doi.org/10.1002/esp.1031

Gasparini, N.M., Whipple, K.X. & Bras, R.L. (2007) Predictions of steady state and transient landscape morphology using sediment-flux-dependent river incision models. *Journal of Geophysical Research - Earth Surface*, 112(F3). https://doi.org/10.1029/2006JF000567

Gonzalez, M., Clavel, F., Christiansen, R., Gianni, G.M., Lince Klinger, F., Martinez, P. *et al.* (2020) The Iglesia basin in the southern Central Andes: A record of backarc extension before wedge-top deposition in a foreland basin. *Tectonophysics*, 792, 228590. https://doi.org/10.1016/j.tecto.2020.228590

Goren, L., Fox, M. & Willett, S.D. (2014) Tectonics from fluvial topography using formal linear inversion: Theory and applications to the Inyo Mountains, California. *Journal of Geophysical Research, F: Earth Surface*, 119(8), 1651–1681. https://doi.org/10.1002/2014JF003079

Harbor, J. & Warburton, J. (2006) Relative rates of glacial and nonglacial erosion in Alpine environments. *Arctic and Alpine Research*, 25(1), 1. https://doi.org/10.2307/1551473

Harries, R.M., Kirstein, L.A., Whittaker, A.C., Attal, M., Peralta, S. & Brooke, S. (2018) Evidence for self-similar Bedload transport on Andean alluvial fans, Iglesia Basin, south Central Argentina. *Journal of Geophysical Research - Earth Surface*, 123(9), 2292–2315. https://doi.org/10.1029/2017JF004501

Harries, R.M., Kirstein, L.A., Whittaker, A.C., Attal, M. & Main, I. (2019) Impact of recycling and lateral sediment input on grain size fining trends—Implications for reconstructing tectonic and climate forcings in ancient sedimentary systems. *Basin Research*, 31(5), 866–891. https://doi.org/10.1111/bre.12349

Hergarten, S., Robl, J. & Stuwe, K. (2016) Tectonic geomorphology at small catchment sizes-extensions of the stream-power approachand the x method. *Earth Surface Dynamics*, 4(1), 1–9. https://doi.org/10.5194/esurf-4-1-2016

Hobley, D.E.J., Sinclair, H.D., Mudd, S.M. & Cowie, P.A. (2011) Field calibration of sediment flux dependent river incision. *Journal of Geophysical Research - Earth Surface*, 116(F4). https://doi.org/10.1029/2010JF001935

Hodge, R.A., Hoey, T.B. & Sklar, L.S. (2011) Bed load transport in bedrock rivers: The role of sediment cover in grain entrainment, translation, and deposition. *Journal of Geophysical Research - Earth Surface*, 116(F4). https://doi.org/10.1029/2011JF002032

Hoke, G.D., Giambiagi, L.B., Garzione, C.N., Mahoney, J.B. & Strecker, M.R. (2014) Neogene paleoelevation of intermontane basins in a narrow, compressional mountain range, southern Central Andes of Argentina. *Earth and Planetary Science Letters*, 406, 153–164. https://doi.org/10.1016/j.epsl.2014.08.032

Hooke, J. (2003) Coarse sediment connectivity in river channel systems: A conceptual framework and methodology. *Geomorphology*, 56(1-2), 79–94. https://doi.org/10.1016/S0169-555X(03)00047-3

Hurst, M.D., Mudd, S.M., Walcott, R., Attal, M. & Yoo, K. (2012) Using hilltop curvature to derive the spatial distribution of erosion rates. *Journal of Geophysical Research - Earth Surface*, 117(F2). https://doi.org/10.1029/2011JF002057

Hurst, M.D., Mudd, S.M., Yoo, K., Attal, M. & Walcott, R. (2013) Influence of lithology on hillslope morphology and response to tectonic forcing in the northern Sierra Nevada of California. *Journal of Geophysical Research - Earth Surface*, 118(2), 832–851. https://doi.org/10.1002/jgrf.20049

Jeffery, M.L., Yanites, B.J., Poulsen, C.J. & Ehlers, T.A. (2014) Vegetation-precipitation controls on central Andean topography. *Journal of Geophysical Research - Earth Surface*, 119(6), 1354–1375. https://doi.org/10.1002/2013JF002919

Jerolmack, D.J. & Paola, C. (2010) Shredding of environmental signals by sediment transport. *Geophysical Research Letters*, 37(19). https://doi.org/10.1029/2010GL044638

Johnstone, S.A. & Hilley, G.E. (2015) Lithologic control on the form of soil-mantled hillslopes. *Geology*, 43(1), 83–86. https://doi.org/10.1130/G36052.1

Jones, R.E., Kirstein, L.A., Kasemann, S.A., Litvak, V.D., Poma, S., Alonso, R.N. *et al.* (2016) The role of changing geodynamics in the progressive contamination of late cretaceous to Late Miocene arc magmas in the southern Central Andes. *Lithos*, 262, 169–191. https://doi.org/10.1016/j.lithos.2016.07.002

Jordan, T.E., Allmendinger, R.W., Damanti, J.F. & Drake, R.E. (1993) Chronology of motion in a complete Thrust Belt: The Precordillera, 30-31°S, Andes Mountains. *The Journal of Geology*, 101(2), 135–156. https://doi.org/10.1086/648213

Kirby, E. & Whipple, K.X. (2012) Expression of active tectonics in erosional landscapes. *Journal of Structural Geology*, 44, 54–75. https://doi.org/10.1016/j.jsg.2012.07.009

Kirstein, L.A., Carter, A. & Chen, Y.G. (2010) Testing inferences from palaeocurrents: Application of zircon double-dating to Miocene sediments from the Hengchun peninsula, Taiwan. *Terra Nova*, 22(6), 483–493. https://doi.org/10.1111/j.1365-3121.2010.00970.x

Koppes, M., Hallet, B., Rignot, E., Mouginot, J., Wellner, J.S. & Boldt, K. (2015) Observed latitudinal variations in erosion as a function of glacier dynamics. *Nature*, 526(7571), 100–103. https://doi.org/10.1038/nature15385

Korup, O. & Montgomery, D.R. (2008) Tibetan plateau river incision inhibited by glacial stabilization of the Tsangpo gorge. *Nature*, 455(7214), 786–789. https://doi.org/10.1038/nature07322

Korup, O., Montgomery, D.R. & Hewitt, K. (2010) Glacier and landslide feedbacks to topographic relief in the Himalayan syntaxes. *Proceedings of the National Academy of Sciences of the United States of America*, 107(12), 5317–5322. https://doi.org/10.1073/pnas.0907531107

Lane, S.N., Bakker, M., Gabbud, C., Micheletti, N. & Saugy, J.N. (2017) Sediment export, transient landscape response and catchment-scale connectivity following rapid climate warming and Alpine glacier recession. *Geomorphology*, 277, 210–227. https://doi.org/10.1016/j.geomorph.2016.02.015

Lavarini, C., Attal, M., da Costa Filho, C.A. & Kirstein, L.A. (2018) Does pebble abrasion influence detrital age population statistics? A numerical investigation of natural data sets. *Journal of Geophysical Research - Earth Surface*, 123(10), 2577–2601. https://doi.org/10.1029/2018JF004610

Li, G., West, A.J., Densmore, A.L., Hammond, D.E., Jin, Z. *et al.* (2016) Connectivity of earthquake-triggered landslides with the fluvial network: Implications for landslide sediment transport after the 2008 Wenchuan earthquake. *Journal of Geophysical Research - Earth Surface*, 121(4), 703–724. https://doi.org/10.1002/2015JF003718

Litty, C., Lanari, P., Burn, M. & Schlunegger, F. (2017) Climate-controlled shifts in sediment provenance inferred from detrital zircon ages, western Peruvian Andes. *Geology*, 45(1), 59–62. https://doi.org/10.1130/G38371.1

Litty, C., Schlunegger, F., Akçar, N., Delunel, R., Christl, M. & Vockenhuber, C. (2018) Chronology of alluvial terrace sediment accumulation and incision in the Pativilca Valley, western Peruvian Andes. *Geomorphology*, 315, 45–56. https://doi.org/10.1016/j.geomorph.2018.05.005

Lukens, C.E., Riebe, C.S., Sklar, L.S. & Shuster, D.L. (2016) Grain size bias in cosmogenic nuclide studies of stream sediment in steep terrain. *Journal of Geophysical Research - Earth Surface*, 121(5), 978–999. https://doi.org/10.1002/2016JF003859

Lukens, C.E., Riebe, C.S., Sklar, L.S. & Shuster, D.L. (2020) Sediment size and abrasion biases in detrital thermochronology. *Earth and Planetary Science Letters*, 531, 115929. https://doi.org/10.1016/j.epsl.2019.115929

MacGregor, K.R., Anderson, R.S. & Waddington, E.D. (2009) Numerical modeling of glacial erosion and headwall processes in alpine valleys. *Geomorphology*, 103(2), 189–204. https://doi.org/10.1016/j.geomorph.2008.04.022

MacGregor, K.R., Anderson, R.S., Anderson, S.P. & Waddington, E.D. (2000) Numerical simulations of glacial-valley longitudinal profile evolution. *Geology*, 28(11), 1031–1034. https://doi.org/10.1130/0091-7613(2000)028<1031:NSOGVL>2.3.CO;2

Malatesta, L.C. & Avouac, J.P. (2018) Contrasting river incision in north and South Tian Shan piedmonts due to variable glacial imprint in mountain valleys. *Geology*, 46(7), 659–662. https://doi.org/10.1130/G40320.1

Malatesta, L.C., Avouac, J.P., Brown, N.D., Breitenbach, S.F.M., Pan, J., Chevalier, M.L. *et al.* (2018) Lag and mixing during sediment transfer across the Tian Shan piedmont caused by climate-driven aggradation–incision cycles. *Basin Research*, 30(4), 613–635. https://doi.org/10.1111/bre.12267

Martinod, J., Gérault, M., Husson, L. & Regard, V. (2020) Widening of the Andes: An interplay between subduction dynamics and crustal wedge tectonics. *Earth-Science Reviews*, 204, 103170. https://doi.org/10.1016/j.earscirev.2020.103170

Mather, A.E., Stokes, M. & Whitfield, E. (2017) River terraces and alluvial fans: The case for an integrated quaternary fluvial archive. *Quaternary Science Reviews*, 166, 74–90. https://doi.org/10.1016/j.quascirev.2016.09.022

Meigs, A., Krugh, W.C., Davis, K. & Bank, G. (2006) Ultra-rapid landscape response and sediment yield following glacier retreat, Icy Bay, southern Alaska. *Geomorphology*, 78(3-4), 207–221. https://doi.org/10.1016/j.geomorph.2006.01.029

Micheletti, N. & Lane, S.N. (2016) Water yield and sediment export in small, partially glaciated Alpine watersheds in a warming climate. *Water Resources Research*, 52(6), 4924–4943. https://doi.org/10.1002/2016WR018774

Mishra, K., Sinha, R., Jain, V., Nepal, S. & Uddin, K. (2019) Towards the assessment of sediment connectivity in a large Himalayan river basin. *The Science of the Total Environment*, 661, 251–265. https://doi.org/10.1016/j.scitotenv.2019.01.118

Molnar, P. (2001) Climate change, flooding in arid environments, and erosion rates. *Geology*, 29(12), 1071. https://doi.org/10.1130/0091-7613(2001)029<1071:CCFIAE>2.0.CO

Molnar, P. (2004) Late Cenozoic increase in accumulation rates of terrestrial sediment: How might climate change have affected erosion rates? *Annual Review of Earth and Planetary Sciences*, 32(1), 67–89. https://doi.org/10.1146/annurev.earth.32.091003.143456

Montgomery, D.R. & Korup, O. (2011) Preservation of inner gorges through repeated Alpine glaciations. *Nature Geoscience*, 4(1), 62–67. https://doi.org/10.1038/ngeo1030

Morisawa, M.E. (1962) Quantitative geomorphology of some watersheds in the appalachian plateau. *Bulletin Geological Society of America*, 73(9), 1025. https://doi.org/10.1130/0016-7606(1962)73[1025:QGOSWI]2.0.CO;2

Mudd, S.M., Attal, M., Milodowski, D.T., Grieve, S.W.D. & Valters, D.A. (2014) A statistical framework to quantify spatial variation in channel gradients using the integral method of channel profile analysis. *Journal of Geophysical Research - Earth Surface*, 119(2), 138–152. https://doi.org/10.1002/2013JF002981

Mudd, S.M., Clubb, F.J., Gailleton, B. & Hurst, M.D. (2018) How concave are river channels? *Earth Surface Dynamics*, 6(2), 505–523. https://doi.org/10.5194/esurf-6-505-2018

Norton, K.P., Schlunegger, F. & Litty, C. (2016) On the potential for regolith control of fluvial terrace formation in semi-arid escarpments. *Earth Surface Dynamics*, 4(1), 147–157. https://doi.org/10.5194/esurf-4-147-2016

Pedersen, V.K., Egholm, D.L. & Nielsen, S.B. (2010) Alpine glacial topography and the rate of rock column uplift: A global perspective. *Geomorphology*, 122(1-2), 129–139. https://doi.org/10.1016/j.geomorph.2010.06.005

Perucca, L.P. & Martos, L.M. (2012) Geomorphology, tectonism and Quaternary landscape evolution of the Central Andes of San Juan (30°S-69°W), Argentina. *Quaternary International*, 253, 80–90. https://doi.org/10.1016/j.quaint.2011.08.009

Pfeiffer, A.M., Collins, B.D., Anderson, S.W., Montgomery, D.R. & Istanbulluoglu, E. (2019) River bed elevation variability reflects sediment supply, rather than peak flows, in the uplands of Washington State. *Water Resources Research*, 55(8), 6795–6810. https://doi.org/10.1029/2019WR025394

Prasicek, G., Hergarten, S., Deal, E., Herman, F. & Robl, J. (2020) A glacial buzzsaw effect generated by efficient erosion of temperate glaciers in a steady state model. *Earth and Planetary Science Letters*, 543, 116350. https://doi.org/10.1016/j.epsl.2020.116350

Quick, L., Sinclair, H.D., Attal, M. & Singh, V. (2019) Conglomerate recycling in the Himalayan foreland basin: Implications for grain size and provenance. *GSA Bulletin*, 132(7-8), 1639–1656. https://doi.org/10.1130/b35334.1

Rainato, R., Picco, L., Cavalli, M., Mao, L., Neverman, A.J. & Tarolli, P. (2018) Coupling climate conditions, sediment sources and sediment transport in an Alpine Basin. *Land Degradation and Development*, 29(4), 1154–1166. https://doi.org/10.1002/ldr.2813

Ramos, V.A., Cristallini, E.O. & Pérez, D.J. (2002) The Pampean flat-slab of the Central Andes. *Journal of South American Earth Sciences*, 15(1), 59–78. https://doi.org/10.1016/S0895-9811(02)00006-8

Reinhardt, L.J., Hoey, T.B., Barrows, T.T., Dempster, T.J., Bishop, P. & Fifield, L.K. (2007) Interpreting erosion rates from cosmogenic radionuclide concentrations measured in rapidly eroding terrain. *Earth Surface Processes and Landforms*, 32(3), 390–406. https://doi.org/10.1002/esp.1415

Riebe, C.S., Sklar, L.S., Lukens, C.E. & Shuster, D.L. (2015) Climate and topography control the size and flux of sediment produced on steep mountain slopes. *Proceedings of the National Academy of Sciences*, 112(51), 15574–15579. https://doi.org/10.1073/pnas.1503567112

Riesner, M., Simoes, M., Carrizo, D. & Lacassin, R. (2019) Early exhumation of the frontal cordillera (southern Central Andes) and implications for Andean mountain-building at ∼33.5°S. *Scientific Reports*, 9(1), 7972. https://doi.org/10.1038/s41598-019-44320-1

Roda-Boluda, D.C., D'Arcy, M., McDonald, J. & Whittaker, A.C. (2018) Lithological controls on hillslope sediment supply: Insights from landslide activity and grain size distributions. *Earth Surface Processes and Landforms*, 43(5), 956–977. https://doi.org/10.1002/esp.4281

Royden, L., Clark, M.K. & Whipple, K.X. (2000) Evolution of river elevation profiles by bedrock incision; analytical solutions for transient river profiles related to changing uplift and precipitation rates. *Eos, Transactions of the American Geophysical Union*, 81. Abstract T62F-09.

Royden, L. & Taylor Perron, J. (2013) Solutions of the stream power equation and application to the evolution of river longitudinal profiles. *Journal of Geophysical Research - Earth Surface*, 118(2), 497–518. https://doi.org/10.1002/jgrf.20031

Schildgen, T.F., Robinson, R.A.J., Savi, S., Phillips, W.M., Spencer, J.Q.G., Bookhagen, B. *et al.* (2016) Landscape response to late Pleistocene climate change in NW Argentina: Sediment flux modulated by basin geometry and connectivity. *Journal of Geophysical Research - Earth Surface*, 121(2), 392–414. https://doi.org/10.1002/2015JF003607

Siame, L.L., Bourlès, D.L., Sébrier, M., Bellier, O., Carlos Castano, J., Araujo, M. *et al.* (1997) Cosmogenic dating ranging from 20 to 700 ka of a series of alluvial fan surfaces affected by the El Tigre fault, Argentina. *Geology*, 25(11), 975. https://doi.org/10.1130/0091-7613(1997)025<0975:CDRFTK>2.3.CO;2

Steffen, D., Schlunegger, F. & Preusser, F. (2009) Drainage basin response to climate change in the Pisco valley, Peru. *Geology*, 37(6), 491–494. https://doi.org/10.1130/G25475A.1

Stock, J. & Dietrich, W.E. (2003) Valley incision by debris flows: Evidence of a topographic signature. *Water Resources Research*, 39(4). https://doi.org/10.1029/2001WR001057

Stutenbecker, L., Costa, A. & Schlunegger, F. (2016) Lithological control on the landscape form of the upper Rhoˆne basin, central Swiss Alps. *Earth Surface Dynamics*, 4(1), 253–272. https://doi.org/10.5194/esurf-4-253-2016

Tofelde, S., Schildgen, T.F., Savi, S., Pingel, H., Wickert, A.D., Bookhagen, B. *et al.* (2017) 100 kyr fluvial cut-and-fill terrace cycles since the middle Pleistocene in the southern Central Andes, NW Argentina. *Earth and Planetary Science Letters*, 473, 141–153. https://doi.org/10.1016/j.epsl.2017.06.001

Tofelde, S., Savi, S., Wickert, A.D., Bufe, A. & Schildgen, T.F. (2019) Alluvial channel response to environmental perturbations: Fill-terrace formation and sediment-signal disruption. *Earth Surface Dynamics*, 7(2), 609–631. https://doi.org/10.5194/esurf-7-609-2019

Tucker, G.E. & Slingerland, R. (1997) Drainage basin responses to climate change. *Water Resources Research*, 33(8), 2031–2047. https://doi.org/10.1029/97WR00409

Watkins, S.E., Whittaker, A.C., Bell, R.E., Brooke, S.A.S., Ganti, V. *et al.* (2020) Straight from the source's mouth: Controls on field-constrained sediment export across the entire active Corinth Rift, Central Greece. *Basin Research*, 32(6), 1600–1625. https://doi.org/10.1111/bre.12444

Whitbread, K., Jansen, J., Bishop, P. & Attal, M. (2015) Substrate, sediment, and slope controls on bedrock channel geometry in postglacial streams. *Journal of Geophysical Research - Earth Surface*, 120(5), 779–798. https://doi.org/10.1002/2014JF003295

Whittaker, A.C., Attal, M. & Allen, P.A. (2010) Characterising the origin, nature and fate of sediment exported from catchments perturbed by active tectonics. *Basin Research*, 22(6), 809–828. https://doi.org/10.1111/j.1365-2117.2009.00447.x

Whittaker, A.C., Duller, R.A., Springett, J., Smithells, R.A., Whitchurch, A.L. & Allen, P.A. (2011) Decoding downstream trends in stratigraphic grain size as a function of tectonic subsidence and sediment supply. *Bulletin Geological Society of America*, 123(7-8), 1363–1382. https://doi.org/10.1130/B30351.1

Wickert, A.D. & Schildgen, T.F. (2019) Long-profile evolution of transport-limited gravel-bed rivers. *Earth Surface Dynamics*, 7(1), 17–43. https://doi.org/10.5194/esurf-7-17-2019

Wobus, C., Whipple, K.X., Kirby, E., Snyder, N., Johnson, J. *et al.* (2006) Tectonics from topography: Procedures, promise, and pitfalls. *Special Paper of the Geological Society of America*, 398, 55. https://doi.org/10.1130/2006.2398(04)

Zevenbergen, L.W. & Thorne, C.R. (1987) Quantitative analysis of land surface topography. *Earth Surface Processes and Landforms*, 12(1), 47–56. https://doi.org/10.1002/esp.3290120107

Zondervan, J.R., Whittaker, A.C., Bell, R.E., Watkins, S.E., Brooke, S.A.S. & Hann, M.G. (2020) New constraints on bedrock erodibility and landscape response times upstream of an active fault. *Geomorphology*, 351, 106937. https://doi.org/10.1016/j.geomorph.2019.106937

How to cite this article: Harries RM, Gailleton B, Kirstein LA, Attal M, Whittaker AC, Mudd SM. Impact of climate on landscape form, sediment transfer and the sedimentary record. *Earth Surf. Process. Landforms*. 2021;1–18. https://doi.org/10.1002/esp.5075